LAND SUBSIDENCE
Proceedings of the Seventh International Symposium on Land Subsidence
Shanghai China 23 ~ 28 October 2005

SIMULATION OF SUBSIDENCE FOR THE REGIONAL-AQUIFER SYSTEM IN THE SANTA CLARA VALLEY, CALIFORNIA

Randall T. HANSON, Zhen LI, Claudia FAUNT
USGS, 5735 Kearny Villa Road,
San Diego, CA 92123, USA
rthanson@usgs.gov; zhenli@usgs.gov; ccfaunt@usgs.gov

Abstract

Historic ground-water overdraft in the Santa Clara Valley caused up to 3.9 m (12.7 ft) of land subsidence from 1916 to 1969. Importation of water, artificial recharge, and reduced pumpage have resulted in recent land subsidence that is predominantly elastic during seasonal and climatic cycles. However, the need for continual management of the water resources remains. The U.S. Geological Survey (USGS) developed a regional model of ground-water flow and land-subsidence using MODFLOW to assess the effects of changes in the quantity and distribution of recharge and pumpage on regional land subsidence, and to provide the management tool needed to help steward the water resources.

New data were used to develop the simulation model of ground-water flow and subsidence. Inelastic and elastic specific storage values were based on consolidation tests of selected cores from new multi-well monitoring sites. These data suggest that the zones of greatest pumpage are generally less compressible. The measured extensometer data and related wellbore-flow and thermal gradient data indicate that most of the pumpage and subsidence is occurring between 300 and 650 feet blow land surface.

Model simulations match compaction related to seasonal and climate cycles measured at several extensometers, as well as measured ground-water levels and streamflow. The explicit simulation of multi-aquifer wells significantly affects the distribution of layer-specific simulated compaction because intra-wellbore flow from upper-aquifer layers supplies some of the water that otherwise would have been simulated as water from aquifer and aquitard storage in the lower model layers.

Keywords: ground water, subsidence, model, extensometer, pumpage

1. INTRODUCTION

The regional aquifer system formed by the alluvial deposits of the Santa Clara Valley, California (Fig.1) is composed of multiple aquifers and is typical of most regional flow systems in the western United States. Historic ground-water overdraft in the Santa Clara Valley caused up to 3.9m (12.7ft) of land subsidence from 1916 to 1969. Starting in the late 1960s, the Santa Clara Valley Water District (SCVWD) began importation of new surface water supplies for direct delivery and artificial recharge. These surface-water deliveries significantly reduced ground-water pumpage, which was driving the historical subsidence, and generally put most of the basin in a long-term water-level recovery. This historic conjunctive development of ground-water and surface-water resources, which is also typical of many regional aquifer systems, and has resulted in increased ground-water flow driven by reduced pumpage from multi-aquifer wells combined with additional infiltration of streamflow and artificial recharge. The development of the ground-water resources in the Santa Clara Valley, California (Fig.1), has included construction of hundreds of multi-aquifer wells and a large system of artificial recharge ponds that help to sustain and replenish the ground-water resources. This type of ground-water development has increased water-level differences and related vertical flow in parts of the regional flow system, which ultimately affects the magnitude as well as the spatial and vertical distribution of land subsidence.

There remains a need to manage the effects of ground-water pumpage, including regional elastic and inelastic land subsidence. The management of the water resources by SCVWD required a more realistic simulation of ground-water flow. The new model used to assess the combined effects of ground-water and surface-water flows includes subsidence, streamflow routing, climatically variable natural recharge, artificial recharge, faults as flow barriers, and pumpage from multi-aquifer wells. The simulation of flow and subsidence uses a six-layer regional ground-water/surface-water flow model with monthly stress periods for the period 1970-1999 (Hanson et al., 2004).

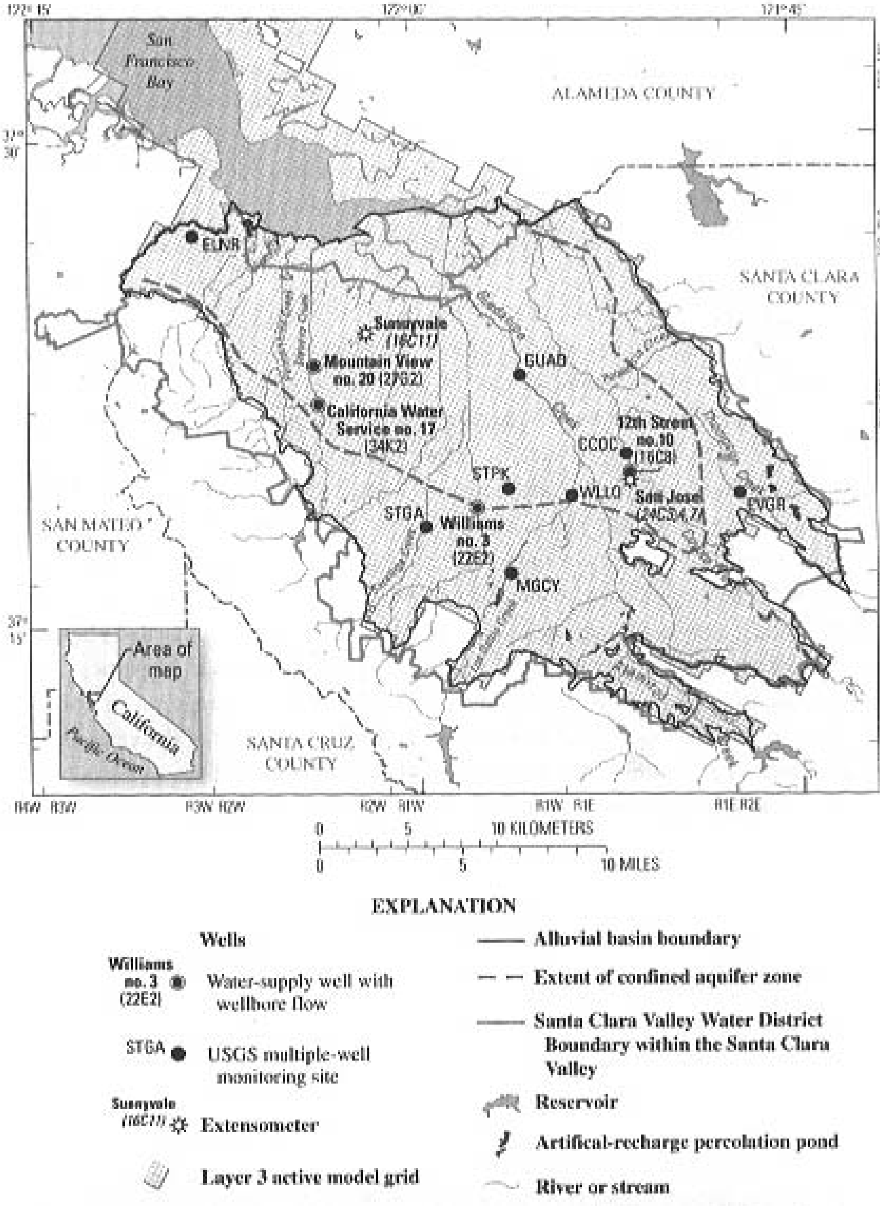

Fig.1 Santa Clara Valley Ground-water flow model, Santa Clara Valley, California

2. SUBSIDENCE PROPERTIES

New data from research drilling were combined with previous geologic and hydrologic information to bet ter estimate the properties needed for the simulation of regional subsidence owing to ground-water pumpage (Hanson et al., 2002; Newhouse et al., 2004). Estimates of skeletal elastic storage co-efficients (S'_{ke}) were based on a combination of estimated values from consolidation tests, extensometers, and reported values (Ireland and others, 1984; Poland and Ireland, 1988; Hanson, 1989). New specific storage values were estimated from consolidation-test data derived from samples of cores from recently completed monitoring-well sites and from recent extensometer data (Fig.1). Skeletal elastic specific storage (S'_{ske}) values from consolidation tests have a geometric mean of 0.4×10^{-5} m^{-1} (1.2×10^{-5} ft^{-1}), with a range from 0.8×10^{-6} m^{-1} to 0.4×10^{-4} m^{-1} (2.7×10^{-6} ft^{-1} to 1.4×10^{-4} ft^{-1}). The graphical estimates of S'_{ke} for data collected from the San Jose and Sunnyvale extensometers for the period 1983-2001 are about 1.2×10^{-3} and 6.2×10^{-3}, respectively (Fig.1). These result in S'_{ske} values on the order of 0.5×10^{-6} m^{-1} and 0.5×10^{-5} m^{-1} (1.5×10^{-6} ft^{-1} and 1.5×10^{-5} ft-1) for San Jose and Sunnyvale, respectively, based on the aggregate thickness of fine-grained de-posits. The S'_{ke} and S'_{ske} estimates for the San Jose extensometer are comparable to the previous estimates reported for the San Jose extensometer of 1.5×10^{-3} for S'ke and 0.6×10^{-6} m^{-1} (1.9×10^{-6} ft^{-1}) for S'_{ske} (Poland and Ireland, 1988), and other reported values for alluvial deposits (Ireland and others, 1984; Hanson, 1989). Even though the geometric mean from con-solidation tests is greater than the value commonly estimated from reported values, it falls within the range of values derived from graphical estimates of local extensometer data.

The new estimates of elastic and inelastic specific-storage values appear to be related to the distribution of wellbore flow (Fig.2). The primary zones where ground water enters the water-supply wells are inferred from the temperature gradient logs from monitoring wells CCOC and GUAD and from the wellbore flow logs from the 12th St. No. 10 and Williams No. 3 water-supply well that is near the CCOC and the GUAD sites, respectively (Hanson et al., 2003; Newhouse et al., 2004). The normal conductive temperature gradients are dis-turbed from a relatively linear and nearly constant value within zones where predominantly lateral ground-water flow is cooling the aquifer and causing selective reductions in the geothermal gradient. Thus the numbered regions shown on figure 2 are zones where lateral ground-water flow is occurring. These zones also are coincident with the sloped parts of the cumulative wellbore flow curves that are zones of lateral ground-water flow in the nearby water-supply wells. These data suggest that repeated pumping cycles may have con-tributed to the preferential reduction of the elastic and inelastic storage properties of the zones with the greatest contribution to wellbore flow. The estimated inelastic specific storage values coincident with the screened/ perforated interval are about 52 (GUAD) to 76 (CCOC) percent of the values above and below screened/perforated interval of greatest wellbore flow. Similarly, the elastic values were about 49 (GUAD) to 88 (CCOC) percent of the zones of reduced pumpage.

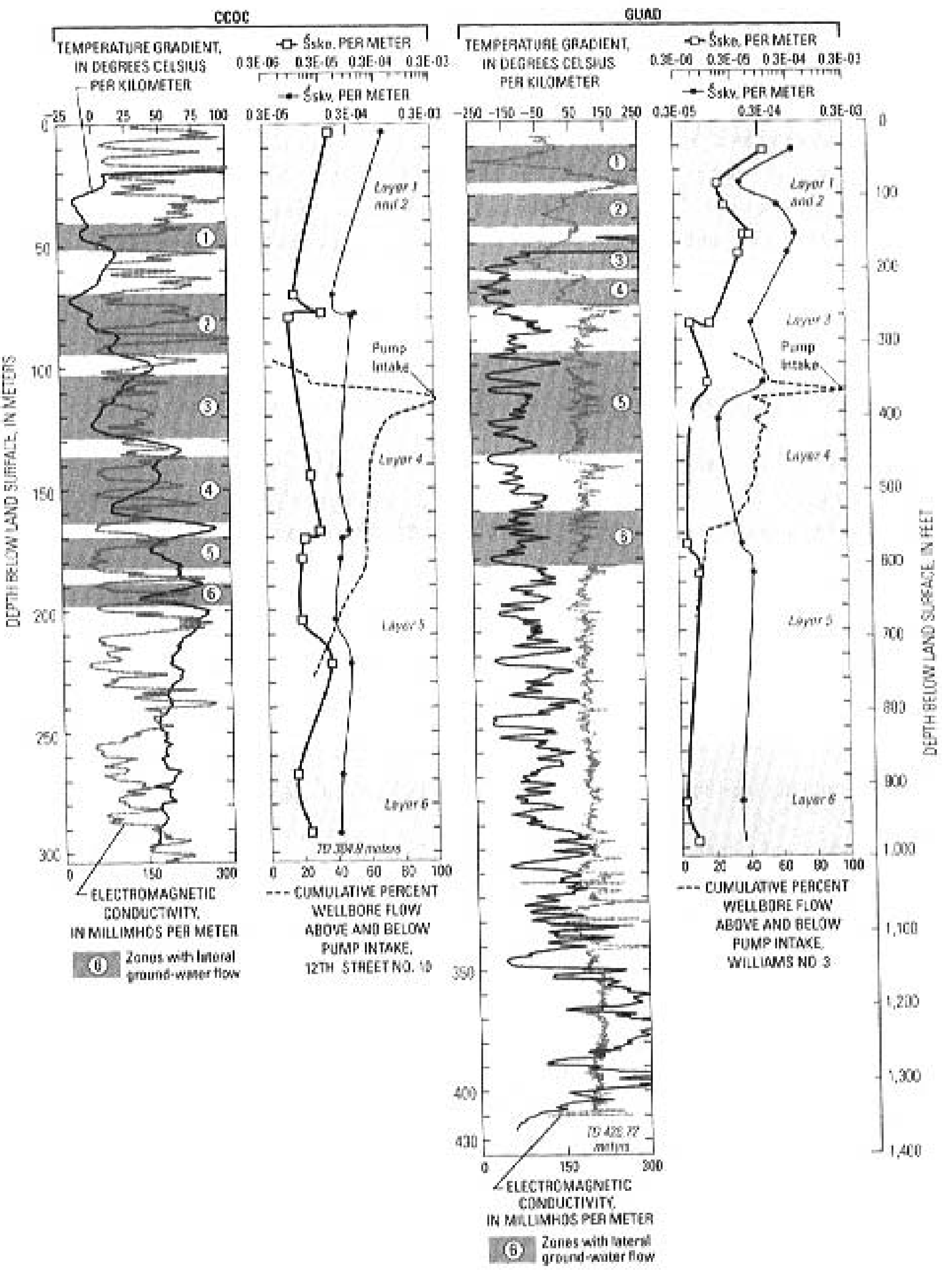

Fig.2 Graph showing the distribution of elastic and inelastic specific storage, and thermal gradient data for CCOC and GUAD monitoring wells and wellbore flow from 12th Street No. 10 and Williams No. 3, Santa Clara Valley, California

Estimates of the elastic and inelastic skeletal storage coefficients are needed to simulate regional subsidence. The regionalized estimates were based on the thickness of sediments of four categories that represent the fractions of model-layer thickness of incompressible coarse-grained (sediment class 4, SC4), incompressible mixed (sediment class 3, SC3), and compressible fine-grained sediments (sediment class 2, SC2) and incompressible fine-grained sediments (sediment class 1, SC1). The values of inelastic storage coefficients were estimated on a cell-by-cell basis as the product of an initial value of the fine-grained interbed elastic skeletal specific storage (S'_{ske}) of 0.9 × 10^{-6} m^{-1} (3.0 × 10^{-6} ft^{-1}) and the aggregate cell-by-cell thickness of the compressible fine-grained deposits (Leighton et al., 1994). For an active model cell in row *i*, column j, and layer *k*, the interbed elastic skeletal storage coefficient was computed as:

$$S'_{ke\ i,j,k} = S'_{ske} \times L_{sc2i,j,k} \quad (1)$$

where,

$S'_{kei,j,k}$ is the interbed elastic skeletal storage coefficient for all fine-grained interbeds in the cell;

S'_{ske} is a common initial value of interbed elastic skeletal specific storage for all model cells for model layer *k* ;

$L_{sc2ij,k}$ is thickness of fine-grained interbeds (sediment class 2, SC2) in the cell.

The composite inelastic skeletal storage coefficient (S'_{skv}) was estimated as the sum of the products of the non-interbed inelastic skeletal specific storage coefficient (S'_{skv}-sc1) of 0.6 × 10^{-6} m^{-1} (2.0 × 10^{-5} ft^{-1}) and the aggregate thickness of coarse-grained sediments (sediment class 4) plus the incompressible fine-grained sediments (sediment class 1) plus the mixed sediments (sediment class 3), and the product of the inelastic specific storage coefficient (S'_{skv}-sc2) of 0.6 × 10^{-4} m^{-1} (2.0 × 10^{-4} ft^{-1}) and the thickness of the compressible fine-grained interbed sediments (sediment class 2) as:

$$S'_{kv\ i,j,k} = (S'_{skv} \times [L_{sc1i,j,k} + L_{sc3i,j,k} + L_{sc4i,j,k}]) + (S'_{skv} \times L_{sc2i,j,k}), \quad (2)$$

where,

S'_{skv} is the common, base initial value of interbed inelastic skeletal specific storage for all model cells for model layer k;

$L_{sc(1\text{-}4)i,j,k}$ refers to the thickness of sediments for categories 4, 3, 2, and 1 and represent the fractions of model-layer thickness of incompressible coarse-grained (sediment class 4, SC4), incompressible mixed (sediment class 3,SC3), and compressible fine-grained sediments (sediment class 2, SC2) and incompressible fine-grained sediments (sediment class 1, SC1), for each cell in each model layer k.

The aggregate cell-by-cell thicknesses of the sedimentary components were interpolated from drillers logs compiled throughout the basin (Leighton et al., 1994). Thus, the resulting elastic storage (fig. 3-1) and inelastic storage (fig. 3-2) coefficients vary spatially with the aggregate thicknesses for each model layer. While uniform values were used initially across all layers, the final calibrated elastic and inelastic specific storage values for the model layers with the majority of pumpage (model layers 3 and 4) were reduced to half the values used for the uppermost and two lowest layers (Hanson and others, 2004).

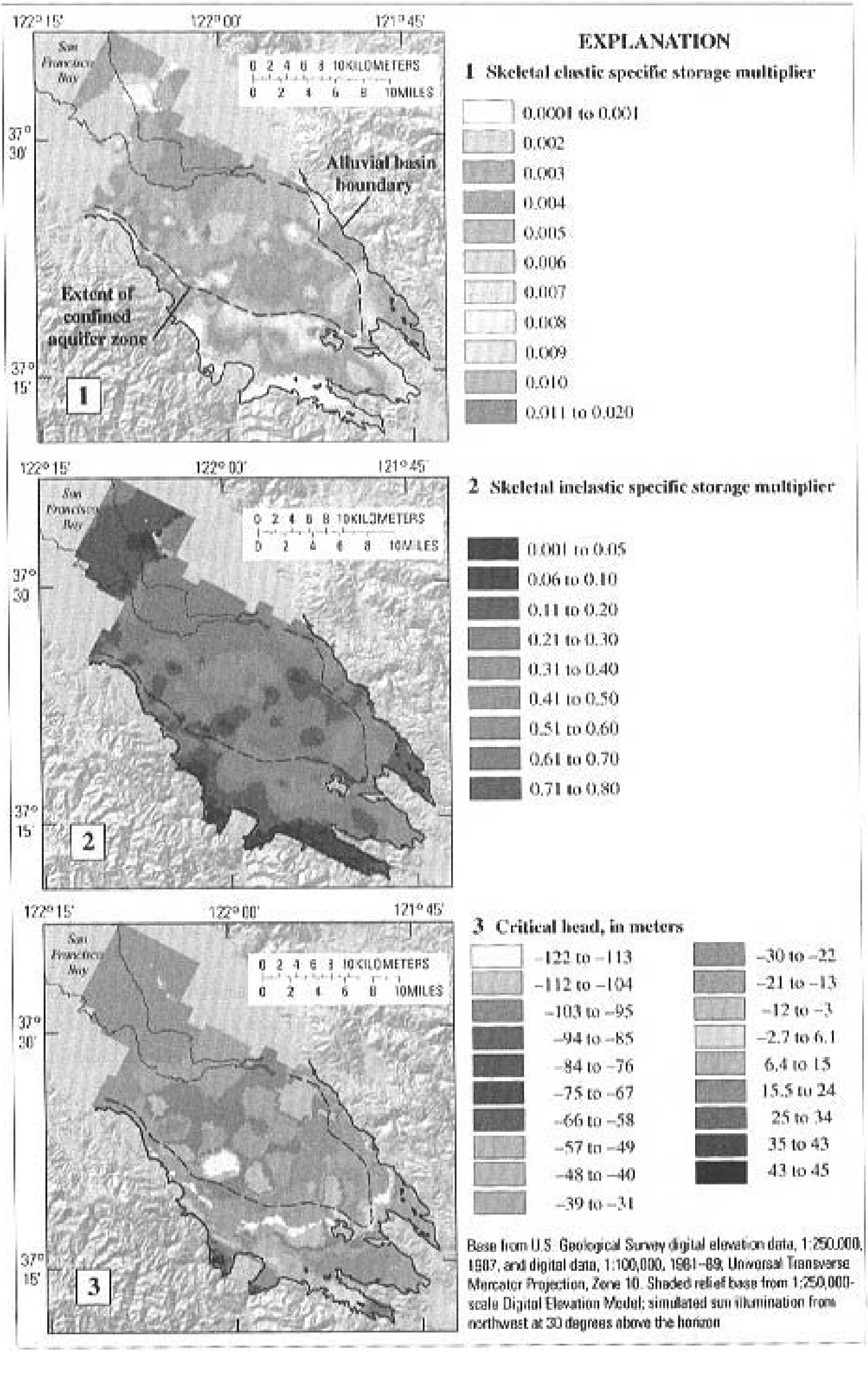

Fig.3 Map showing the distribution of elastic and inelastic storage and critical head for model layer 3, *the Santa Clara Valley, California*

3. SUBSIDENCE SIMULATION

Recent land subsidence is predominantly elastic and occurs over seasonal and climatic cycles. The land subsidence was simulated for all six model layers as ultimate compaction with the Interbed Storage Package (IBS, Leake and Prudic, 1991) in MODFLOW-2000 (MF2K, Harbaugh et al., 2000). This was a reasonable approximation for recent historical deformation since stress-strain relations from extensometer data suggest that all excess pore pressure is dissipated seasonally. The simulated seasonal elastic compaction was as great as 0.03 m (0.11 ft) at the San Jose extensometer (Fig.4) in response to seasonal water-level changes of about 18.3 m (60 ft). This seasonal elastic compaction is superimposed upon longer-term simulated, predominantly elastic compaction of about 0.1m (0.32 ft) from 1983-1989 and recovery (uplift) from 1989-1990 (Fig.4). This multi-year trend is the result of from water-level declines of as much as 35 m (116 ft) during the drought of the late 1980s. Some inelastic compaction may have occurred during the peak summer months of the drought years during maximum water-level declines. Extensometer data from the Sunnyvale site indicates that most of the compaction occurred below the upper extensometer. On the basis of the analysis of wellbore flow and thermal-gradient data from CCOC and GUAD multiple-well monitoring sites, most pumpage occurs within the zone between 300 and 650 ft below land surface (Fig.2), and is coincident with the related compaction at the nearby Sunnyvale extensometer (Fig.4).

Estimates of critical heads were also required for the simulation of subsidence. Critical heads were primarily based on estimates of maximum water level decline (Poland et al., 1988) but were ultimately adjusted during the calibration process. The critical heads were initially set equal to the initial head, with the assumption that the initial heads were representative of January, 1970, conditions, which implies that the fine-grained deposits were normally consolidated at these levels. However, this resulted in anomalous changes in storage and increased water levels during the first few years of the simulation. Critical heads were previously estimated as being 24.4 m (80 ft) lower in 1967 than in 1978 on the basis of the artesian head recovery at the San Jose index well (7S/1E-7R1/6M1; Poland and Ireland, 1988). Thus, the critical heads were then uniformly reset to 80 ft below the initial conditions. Yet a large simulated decrease in head in the peripheral parts of model layer 3 outside a region defined by more than 0.03 m (0.1 ft) of historical subsidence continued creating large contributions from interbed storage and model error. To eliminate this source of error, the critical heads were decreased another 48.8 m (160 ft) in the peripheral areas of model layer 3. In addition, for cells located within the historical cones of depression, the critical heads were increased another 3.04 m (10 ft) to allow for a small amount of inelastic compaction in the late 1980s near the San Jose index well after the dry period in the late 1970s (Fig.3-3). The resulting critical-head values were based on model calibration and may represent a lower bound of critical heads within the basin and within specific model layers. Critical heads remain uncertain in some parts of the basin where simulated subsidence in the southwestern margins is still larger than expected (Fig.3-3, 5). Critical heads may also be uncertain in the pumping centers because water-level declines during the droughts of the simulation period may not have exceeded historical lows.

Calibration of the land subsidence model was constrained by data collected at two extensometers and Interferometric Synthetic Aperture Radar data. The calibrated model matches compaction related to seasonal and climate cycles measured at several extensometers (Fig.4), as well as measured ground-water levels and streamflow. Patterns [simulated subsidence not contoured] of simulated subsidence for the period 1983-1999 are generally aligned with those for historical subsidence (Fig.5) and are in general agreement with the InSAR estimate for seasonal subsidence for January through August 1997 (Galloway, et al., 2000; Hanson et al., 2004). Additional subsidence may be occurring southwest of the historical subsidence bowl due to more recent pumpage (Fig.5). However, this subsidence is likely overestimated due to uncertainty in the critical heads in the southwestern part of the valley.

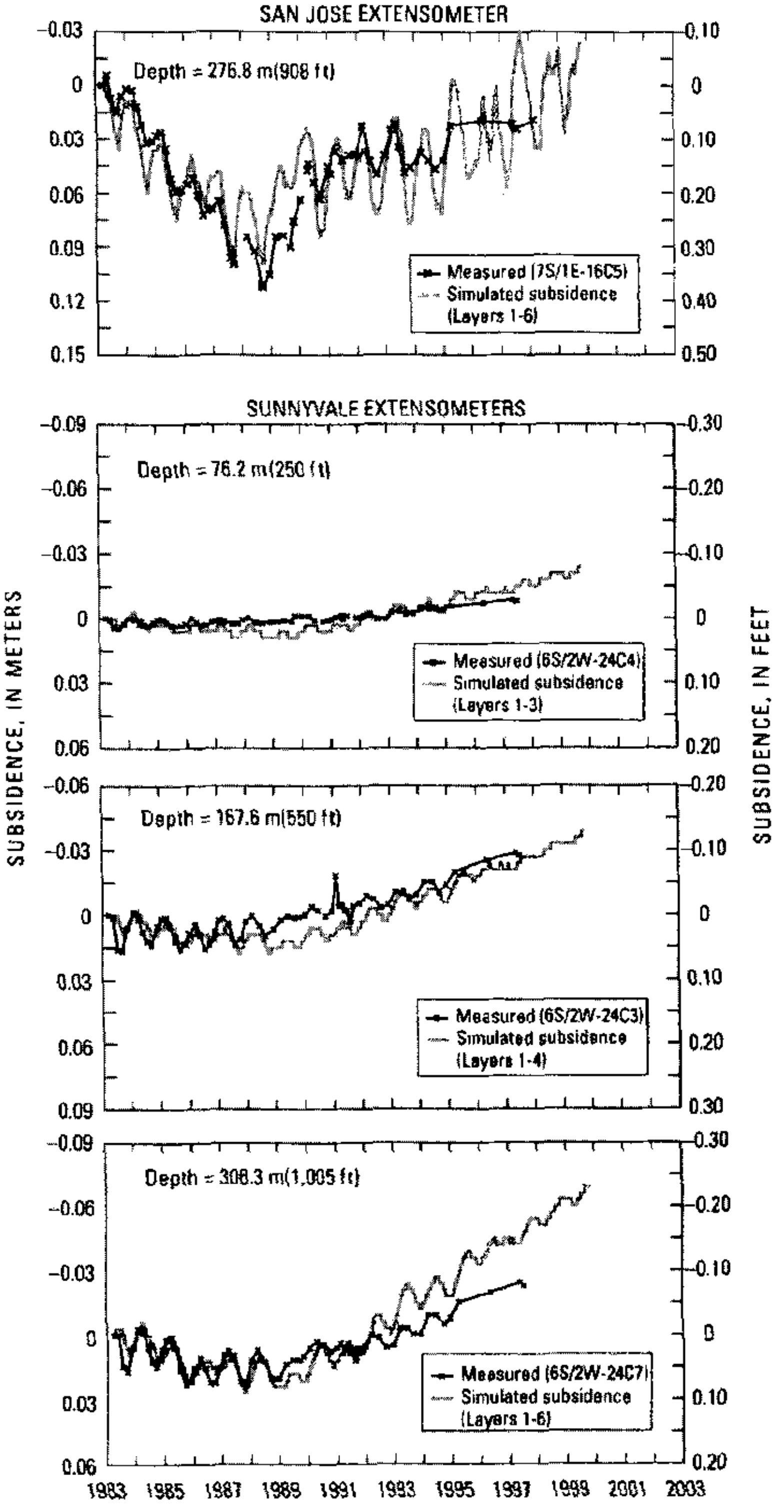

Fig.4 Graph showing measured and simulated compaction for the extensometers at San Jose and Sunnyvale in the Santa Clara Valley, California

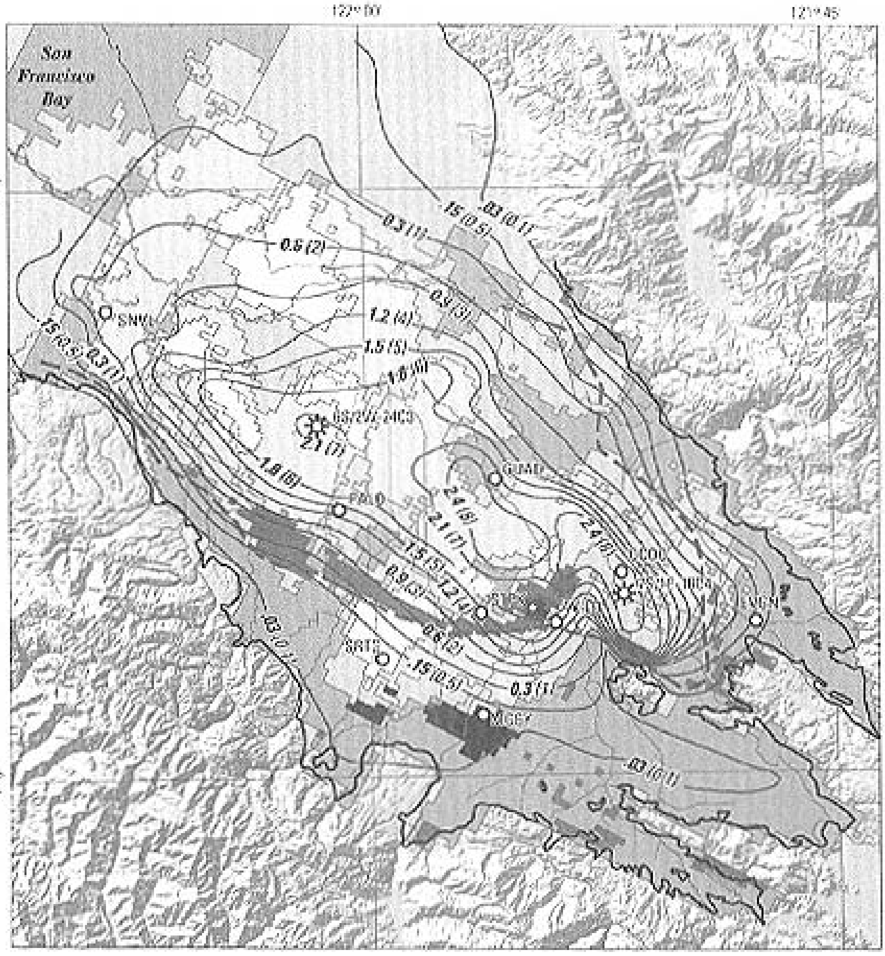

Base from U.S. Geological Survey digital elevation data, 1:250,000, 1987, and digital data, 1:100,000, 1981 89; Universal Transverse Mercator Projection, Zone 10. Shaded relief base from 1:250,000-scale Digital Elevation Model; simulated sun illumination from northwest at 30 degrees above the horizon

0 5 KILOMETERS
0 5 MILES

EXPLANATION

Simulated land subsidence (Jan 1983–Sep 1999) —In meters (feet indicated in parenthesis). Negative number indicates uplift

- −0.19 to −0.09 *(−0.62 to −0.30)*
- −0.088 to −0.06 *(−0.29 to −0.20)*
- −0.058 to −0.03 *(−0.19 to −0.10)*
- −0.027 to 0 *(−0.09 to 0)*
- 0.003 to 0.03 *(0.01 to 0.10)*
- 0.034 to 0.15 *(0.11 to 0.50)*
- 0.155 to 0.457 *(0.51 to 1.50)*
- 0.46 to 0.914 *(1.51 to 3.00)*
- 0.917 to 1.83 *(3.01 to 6.00)*
- 1.83 to 2.74 *(6.01 to 9.00)*

1.5 (2) **Line of measured subsidence (1939-1980)**— In meters (in feet in *parenthesis*). *(Poland and Ireland, 1988)*

Basin boundary

Extent of confined aquifer zone

Creeks

EVGN **Monitoring wells**

8S/2W-24C3 **Extensometers**

Fig.5 Map showing hand-contoured measured subsidence, 1939-1980, and simulated ground compaction, 1983-1999, for the Santa Clara Valley model, Santa Clara Valley, California (Hanson and others, 2004)

4. SUBSIDENCE AND REGIONAL FLOW

Water derived from simulated land subsidence accounts for about one percent of the average net simulated regional ground-water outflow for the period 1970-1999, which includes a drought followed by a decade of sustained recovery. Likewise, this water of compaction accounts for as much as three percent of the simulated pumpage for the drought period 1984-1989. Wellbore-flow and thermal-gradient data indicate that the majority of this water is derived from compaction within the zone between 300 and 650 ft below land surface. This may be due to a reduction in the compressibility of the aquifer system in the zones of major pumpage and (or) the presence of less compressible fine-grained sediments interbedded between the major aquifer layers.

Pumpage from multi-aquifer wells that span up to four model layers, simulated with the MNW package (Halford and Hanson, 2002), significantly affects the distribution of layer-specific simulated compaction. The MNW package allows the simulation of intra-wellbore flow from upper to lower aquifer layers. This water would otherwise have been simulated as being derived from aquifer and aquitard storage in the lower model layers by way of vertical flow through the aquifer system. Thus, simulating multi-aquifer wellbore flow helps separate vertical interaquifer flow through wellbores from flow across the aquifers and fine-grained interbeds. The distribution of simulated flow between model layers has largely shifted from interlayer flow to intrawellbore flow, which represents about 19 percent of the total regional flow. This separation of flows affects the hydrologic budget of the basin, simulated interlayer flow, streamflow infiltration, and in particular the distribution and magnitude of layer-specific compaction (Fig. 6). Multi-aquifer pumpage includes single and multi-layer pumping wells as well as all unpumped and abandoned multi-aquifer wells. Simulated pumpage with the MNW package changes through time with as many as 40 percent single-aquifer wells and 60 percent multi-aquifer wells in 1970, and intrawellbore flow in inactive multi-aquifer wells increases over time, involving a maximum of 40 percent of these wells by 1989 (Hanson et al., 2003). The addition of MNW pumpage allows simulation of more ground water flowing downward from the uppermost layers. This results in increased net streamflow infiltration in the uppermost layers and reduced subsidence in the lower layers (Hanson et al., 2003). The simulation of subsidence is affected by the distribution of wellbore flow and interlayer flow, which changes the relative portions of water derived from aquifer storage, interbed storage, and interaquifer flow. For example, when the simulation uses fixed flows as opposed to multi-aquifer flow, a greater portion of the subsidence is simulated in the deeper model layer 5 (Fig. 6).

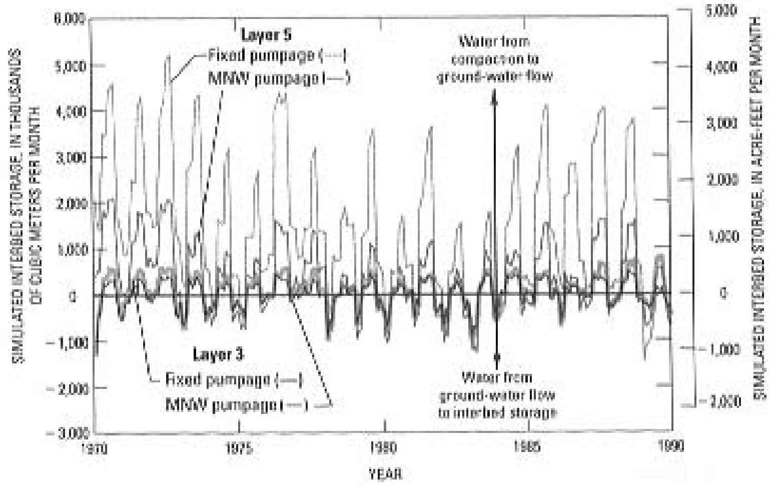

Fig.6 Graph of distribution of simulated interbed storage for model layers 3 and 5 with and without intrawellbore flow, Santa Clara Valley, California

5. SUMMARY

Simulated subsidence in the multi-aquifer regional flow system of the Santa Clara Valley successfully captures subsidence driven by water-level changes over seasonal and climate cycles, matches extensometer data, and is generally in alignment with historical subsidence (Poland and Ireland, 1988) and Interferometric Synthetic Aperture Radar (InSAR) images (Galloway et al., 2000). Simulations indicate that additional subsidence may be occurring from more recent pumpage to the southwest of the historical subsidence bowl. The measured extensometer data and related wellbore-flow and thermal gradient data indicate that most of the pumpage and subsidence is occurring between 300 and 650 feet blow land surface. Consolidation-test data in combination with temperature and wellbore flow data indicates that the compressibility of the aquifer system may have been reduced within this zone and (or) that water is being derived from less compressible fine-grained sediments interbedded between the major aquifer layers. The use of aggregate thicknesses of coarse and fine-grained sediments is a useful approach to estimating storage properties for the simulation of subsidence. The application of the MNW package helps to simulate multi-aquifer flow and affects the simulated vertical distribution of subsidence in the regional ground-water flow system. The new model provides a useful tool for the management of the water resources of the Santa Clara Valley, including the simulation of subsidence throughout the regional aquifer system.

REFERENCES

Galloway, D.L., Jones, D.R., Ingebritsen, S.E., 2000, Measuring land subsidence from space: U.S. Geological Survey Fact Sheet 051-00, 4 p.

Halford, K. J., and Hanson, R.T., 2002. User's Guide User Guide for the Drawdown-Limited, Multi-Node Well (MNW) Package for the U.S. Geological Survey's Modular Three-Dimensional Finite-Difference Ground-Water Flow Model, Versions MODFLOW-96 and MODFLOW-2000, U.S. Geological Survey Open-File Report OFR 02-293, 33 p.

Hanson, R.T., 1989, Aquifer-system compaction, Tucson basin and Avra Valley, Arizona: U.S. Geological Survey Water-Resources Investigations Report 88-4172, 69 p.

Hanson, R.T., Newhouse M.W., Wentworth, C.M., Williams, C.F., Noce, T.E., Bennett, M.J., 2002, Santa Clara Valley Water District multi-aquifer monitoring-well site, Coyote Creek Outdoor Classroom, San Jose, California: U.S. Geological Survey Open-File Report 02-369, 4 p.

Hanson, R.T., Li, Z., and Faunt C., 2003, Application of the multi-node well package to the simulation of regional-aquifer systems in the Santa Clara Valley, California: Modflow and More 2003: Understanding through Modeling- Conference Proceedings, International Ground Water Modeling Center, Golden, CO, September 16-19, 2003 , pp. 74-78

Hanson, R.T., Li, Z., and Faunt C., 2004, Documentation of the Santa Clara Valley regional ground-water/surface-water flow model, Santa Clara County, California: Scientific Investigations Report SIR2004-5231, 75 p. (http://pubs. water.usgs.gov/sir2004-5231/)

Harbaugh, A.W., Banta, E.R., Hill, M.C., and McDonald, M.G., 2000. MODFLOW-2000, The U.S. Geological Survey Modular Ground-Water Model-User Guide to Modularization Concepts and the Ground-Water Flow Process: U.S. Geological Survey Open-File Report OFR 00-92, 121 p.

Ireland R.L., J.F. Poland, and F.S. Riley, 1984, Land Subsidence in the San Joaquin Valley, California, as of 1980: U.S. Geological Survey Professional Paper 437-I, 93 p.

Leake, S.A., and Prudic, D.E., 1991, Documentation of a computer program to simulate aquifer-system compaction using the modular finite-difference ground-water flow model: U.S. Geological Survey Techniques of Water-Resources Investigations, book 6, chap. A2, 68 p.

Leighton, D.A., Fio, J.L., and Metzger, L.F., 1994, Database of well and areal data, South San Francisco Bay and Peninsula area, California: U.S. Geological Survey Water-Resources Investigations Report 94-4151, 47 p.

Newhouse, M.W., Hanson, R.T., Wentworth, C.M., Everett, R., Williams, C. F., Tinsley J., Noce, T. E., and Carkin, B.A. 2004, eologic, water-chemistry, and hydrologic data from multiple-well monitoring sites and selected water-supply wells in the Santa Clara Valley, California, 1999-2003: U.S. Geological Survey Scientific Investigations Report SIR2004-5250, 134 p. (http://pubs.water.usgs.gov/sir2004-5250/)

Poland, J.F., and Ireland R.L., 1988, Land Subsidence in the Santa Clara Valley, California, as of 1982: U.S. Geological Survey Professional Paper 497-F, 61 p.